Proceedings World Geothermal Congress 2015
Melbourne, Australia, 19-25 April 2015

Thermal Remote Sensing at Leyte Geothermal Production Field using Mono-window Algorithms

Serafin Farley M. Meneses III

Geomatics Section, Energy Development Corporation, Philippines

meneses.sm@energy.com.ph

Keywords: Remote Sensing, Land Surface Temperature, Geothermal Exploration

ABSTRACT

Other countries are now using thermal remote sensing as a tool for geothermal energy resource exploration and management. Researchers from Indonesia uses LandSat data to map out potential geothermal sites at Patuha, West Java, Indonesia while researchers from Nevada, USA uses ASTER thermal infrared images to detect and monitor geothermal anomalies within their study area.

In Energy Development Corporation or EDC, thermal remote sensing is introduced as a possible tool for mapping anomalous areas for geothermal exploration by generating land surface temperature (LST) maps using remote sensing datasets. Single channel/Mono-window algorithms were used to generate the LST maps. Two LST maps were derived for Leyte by using 1996- and 2010-acquired LandSat 5 images that are almost cloud free. Agro-meteorological data from the Philippine weather agency were also integrated in the LST map derivation to take into account the climate, weather, and ground conditions during the time the images were captured.

To validate the results that were derived from remote sensing, in-situ ground temperature measurements were conducted using a thermocouple to measure kinematic temperature. Twenty five (25) locations were used to calibrate the data and it was found out that the satellite-derived temperature values gave good correlation with the ground measurements, with variances ranging from 1.52 °C to 3.00 °C.

To complement thermal mapping for future activities, EDC will also look into the possibility of using GIS and geostatistics to use the derived LST maps to determine possible drilling targets by combining the information from the thermal maps with other datasets like structural maps, geophysical maps, and digital elevation models.

1. INTRODUCTION

Other countries are now using Thermal Remote Sensing as an operational tool for geothermal energy resource exploration and management. For instance, research in Indonesia used LandSat data to map a potential geothermal site at Patuha, West Java, Indonesia (Siahaan, Soebandrio and Wikantika 2011). Another research from Nevada, USA used ASTER thermal infrared images to detect and monitor geothermal anomalies within their study area (Coolbaugh, et al. 2007).

Based on the aforementioned and other published researches as case studies, a similar study was conducted by EDC in the Philippine setting with the aim of introducing Land Surface Temperature (LST) mapping using Remote Sensing datasets to identify plausible areas for geothermal exploration. In addition, future aspects of this research will also look into the possibility of using GIS and geostatistics to use the derived LST maps to determine possible target drill locations (i.e. permeable areas) by combining the information from thermal maps with other datasets like structural maps, geophysical maps, and digital elevation models.

2. METHODOLOGY

2.1 Study Area

The study area chosen for this research is the Leyte Geothermal Production Field (LGPF) located at the north central part of Leyte Island situated at the central eastern Visayas Region of the Philippines. LGPF is the world's largest wet steamfield geothermal production field, regularly producing over 700 MW of power. The site is bisected by the northwest trending Philippine Fault and it covers an area of over 15 km^2 of challenging terrain. LGPF was chosen as the study area because of its importance to EDC (i.e. it produces around 60% of the total output of the company) and because the characteristics of the field are relatively well-known already (i.e. it has been operational for almost two-decades).

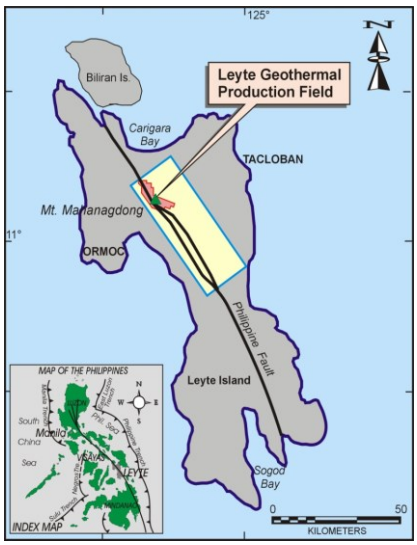

Fig. 1. Location of Leyte Geothermal Production Field or LGPF, central Philippines.

2.2 Remote Sensing Datasets

Since this project is a proof of concept research, only publicly available LandSat 5 datasets were used as sources of thermal infrared data. Satellite images from the LandSat 5 were downloaded via NASA's ECHO|Reverb online facility. For this research, two (2) scenes were used (Fig. 2), chosen for their minimal cloud cover over the subject area.

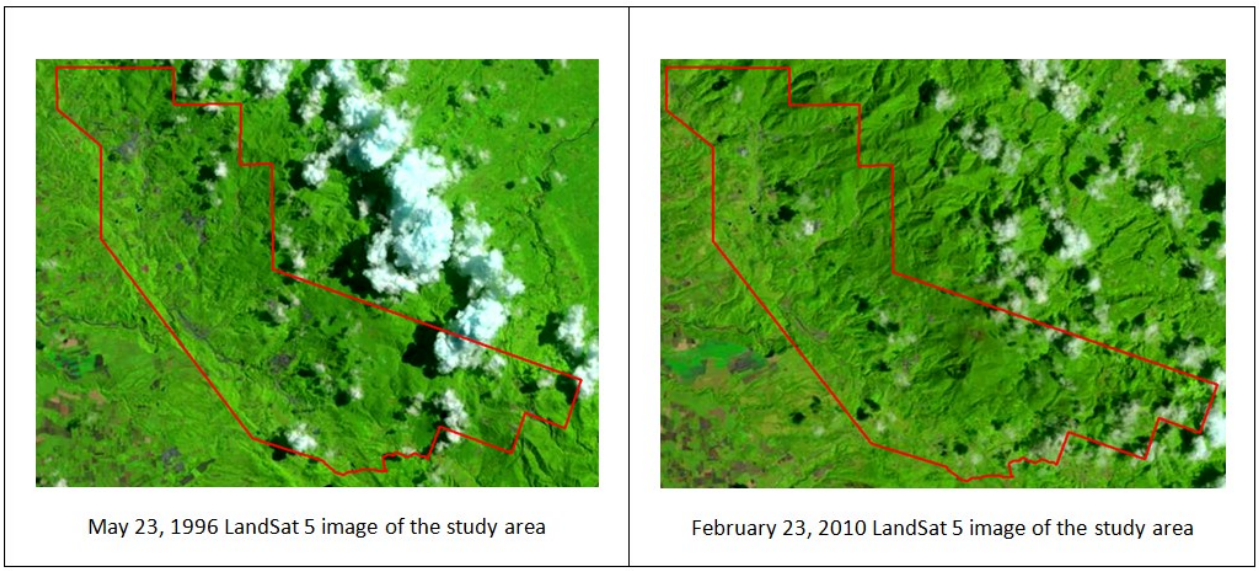

Fig. 2. Available LandSat images over the study area that are almost cloud-free.

Band 6 of LandSat 5 TM was used to generate the thermal maps (Fig. 3) of the study area. The methodologies used to generate the maps will be discussed in Part B below.

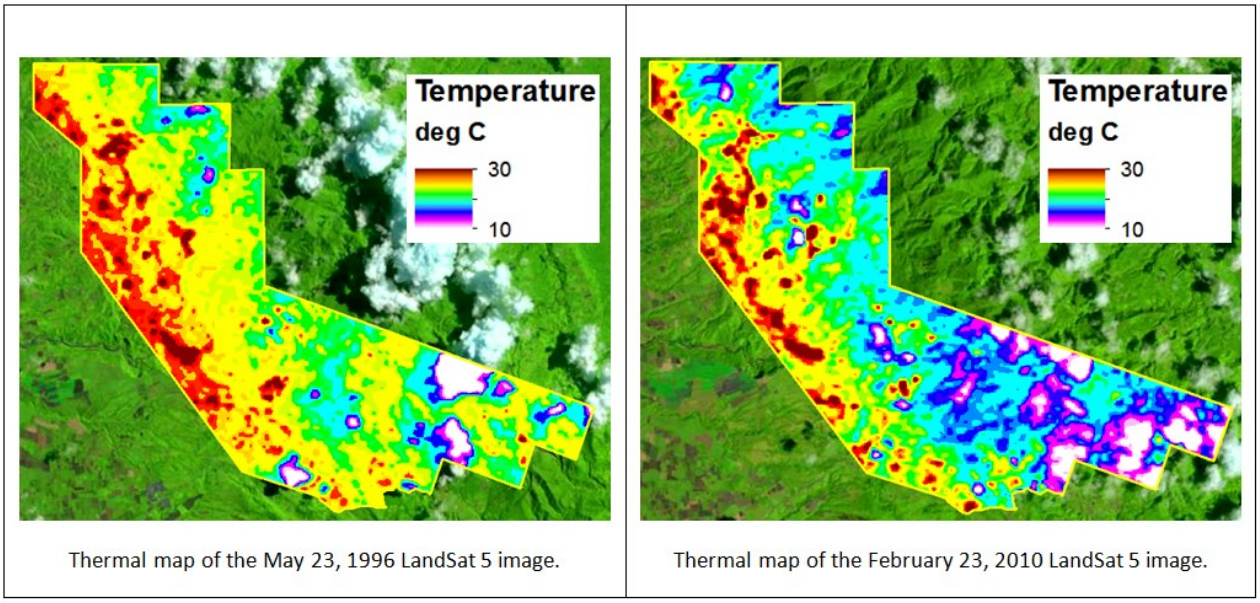

Thermal map of the May 23, 1996 LandSat 5 image.

Thermal map of the February 23, 2010 LandSat 5 image.

Fig. 3. Derived LST maps for the two LandSat datasets used in this research.

Band 6 of LandSat 5 makes use of the thermal infrared region of electromagnetic spectrum (Fig 4). Electromagnetic spectrum refers to the range of all possible values of electromagnetic radiation, either expressed in wavelength or in frequency. When referring to objects, electromagnetic spectrum refers to range of possible frequencies or wavelengths that an object may absorb or emit. These possible spectral values are what the spectrograph onboard the LandSat 5 satellite observes and records when it passes over the study area. Since the objective of the study is to derive LST maps of the study area, band six (wavelength of 10-12 microns) of the LandSat 5 sensor was used.

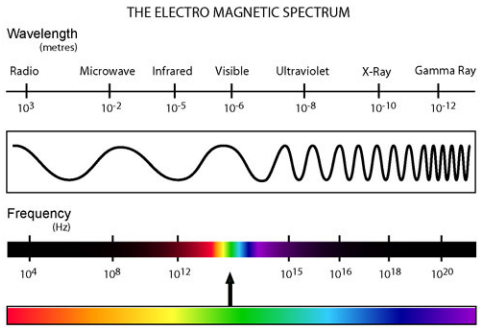

Fig. 4. The electromagnetic spectrum. Adopted from (Shaply 2012).

Since the research is using publicly-available datasets, certain limitations should be expected. Some of these limitations include:

1. Low Temporal Resolution – Repeat pass of LandSat 5 over the Philippines was just every 16 days, there are days that do not have observation data. This means that available LandSat data may not cover all possible seasons in the Philippines (i.e. daily data for the Philippines is not available for download).
2. Medium Spatial Resolution – The re-sampled resolution of LandSat 5 is 30-meters, rendering results better suited for regional analysis.
3. Optical mode of observation – Since the LandSat 5 makes use of 10-12 microns range in the electromagnetic spectrum, thermal images are very susceptible to cloud cover (Fig. 5). This means that most of the available data may be not suitable for analysis due to heavy cloud cover over the study area.

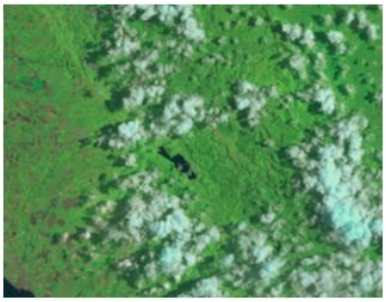

Fig. 5. Sample screen shot of a cloud-covered LandSat 5 image over LGBU, with the unmistakable outline of Lake Danao seen at the middle of the picture.

2.3 Computation Methods

Since LandSat 5 has only one band (i.e. Band 6) suitable for thermal remote sensing, only mono-window or single channel algorithms were used for the study. For this study, three algorithms were considered. The first was NASA methodology (NASA 2013), the second was by Artis and Carnahan (Artis and Carnahan 1982), and the third was by Qin, et. al. (Qin, Karnieli and Berliner 2001).

2.3.1 The "Ideal" Situation – Basics of Thermal Remote Sensing

Before going through the estimation methodologies used in this research, some theoretical background of Thermal Remote Sensing will be discussed to give the reader a condensed primer on the topic and better appreciation of the various methods that will be discussed in subsections.

Thermal Remote Sensing is a technique in the field of Geomatics where Land Surface Temperature or LST maps are derived from aerial or satellite data. Temperature is defined as the concentration of heat energy of a certain matter, while heat energy is the summation of the kinetic energy of randomly moving particles comprising the matter being observed. In order to derive LST maps via Remote Sensing, laws in Physics and Thermodynamics are used as bases. These laws are Planck's Law (Eq. 1), Steffan-Boltzmann Law (Eq. 2), and Wien's Displacement Law (Eq. 3).

$$M = 2\pi hc^2/w^5 \text{ x } (e^{hc/wkT} - 1) \quad (1)$$

$$M = kT^4 \quad (2)$$

$$w = A/T \quad (3)$$

where M is the spectral radiant exitance, h is Planck's constant, c is the speed of light, k is the Steffan-Boltzmann constant, T is absolute temperature, w is wavelength, A is the Wien's constant, respectively.

Planck's Law (Eq. 1) gives the relationship between emitted electromagnetic (EM) radiation from a blackbody at a certain wavelength and its absolute temperature. Steffan-Boltzmann Law (Eq. 2) shows that the total EM radiation emitted by a blackbody is dependent on its absolute temperature. Eq. 3, showing Wien's Displacement Law, describes the maximum wavelength spectral exitance energy with respect to absolute temperature. A blackbody is an ideal theoretical object which translates all of its kinetic energy to thermal energy (i.e. lossless conversion of energy). These laws are used in Remote Sensing to correlate the spectral information gathered by LandSat 5's sixth band (described in section II-A) to land surface temperature.

An ideal scenario to observe LST is shown in Fig. 6. In this case, energy from the sun (represented by a dashed orange line) encounters no obstruction when it travels the atmosphere, down to earth's surface, then towards the spectrograph. Remote Sensing is done by using a system that can avoid clouds (i.e. an airborne system that can fly low to avoid cloud cover), with high temporal, spectral, and spatial resolution. Same-day ground observations are also made using a terrestrial spectrograph and thermocouple. High cost and long duration however, make it difficult to operationalize at such an early stage in the research process. Real world scenario also introduces atmospheric disturbances to Remote Sensing signals. Fig. 7 therefore shows the "optimal" way Thermal Remote Sensing can be done for this study.

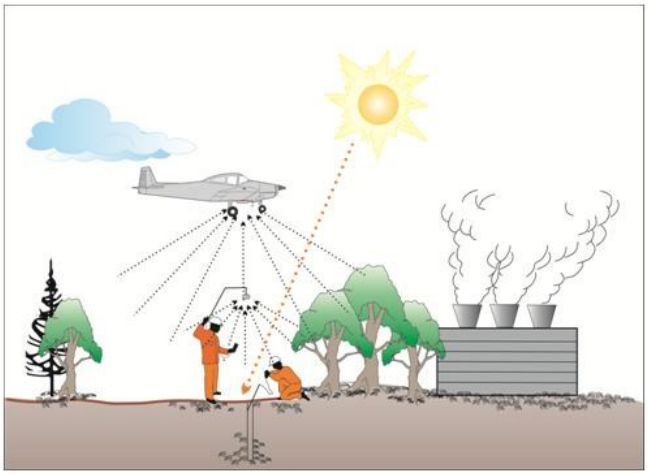

Fig. 6. An "ideal" scenario to do Thermal Remote Sensing. Energy from the sun passes the atmosphere with almost no obstruction and same-day ground observations are also made. Remote Sensing is also done optimally where-in clouds are avoided and the sensor used has high spatial and spectral resolution. Repeat observations can also be made at any given time.

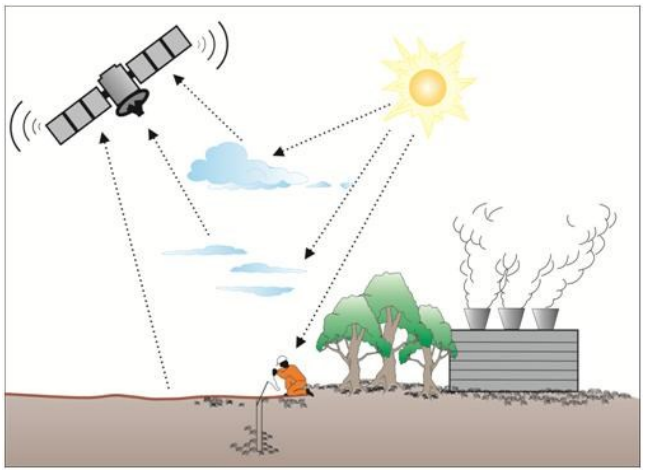

Fig. 7. Actual scenario of doing Thermal Remote Sensing study was done. This research uses LandSat data that is affected by the environmental and systematic sources of errors with no spectral measurements done on ground. Temperature measurements are done years after the image is observed and parametric corrections are sourced from National Aeronautics and Space Administration (NASA), Philippine Atmospheric, Geophysical and Astronomical Services Administration (PAGASA), and from the actual images.

Given that the "ideal" process in determining LST cannot be done in this research, methods that take into account systematic and environmental sources of errors in their solution were found and applied. The first method is the NASA method which takes into account the satellite calibration parameters in solving for LST. Second method is the Artis and Carnahan method which utilizes atmospheric corrections from NASA's online calibration facility. The final method, which that of Qin, et. al., makes use of site-specific correction parameters in deriving the LST. These three methods, which were used in this research, are further discussed below.

2.3.2 The "NASA" Methodology

To get estimated LST values using the NASA method, the following formulae must be used

$$CV = gain \times DN + bias \tag{4}$$

$$CV = ((L_{Max}-L_{Min})/(QCal_{Max}-ACal_{Min})) \times (QCal-QCal_{Min}) + L_{Min} \tag{5}$$

$$T = K_2/\ln(((K_1 \times em)/CV) +1) \tag{6}$$

where CV = cell value radiance, DN = cell value digital number, QCal = digital number, L_{Min} = spectral radiance scaled to $QCal_{Min}$, L_{Max} = spectral radiance scaled to $QCal_{Max}$, K_1 = calibration constant, K_2 = calibration constant, and em for emissivity, respectively.

2.3.3 Artis and Carnahan Technique

Since Eq. 6 gives a temperature with respect to a blackbody response, it can be further improved by using the equation developed by Artis and Carnahan:

$$T_{A\&C} = T/1+(w \times T/p)\ln \tag{7}$$

where $T_{A\&C}$ refers to the LST, corrected for the spectral emissivity of the surface, w is the wavelength of emitted radiance, and p is defined by multiplying Planck's constant with the velocity of light divided by th Boltzmann constant.

2.3.4 Qin et. al.'s Monowindow Algorithm

The final method was that of Qin, et. al. where atmospheric effects were considered in the equations used:

$$T_Q = (a(1-C-D)+(b(1-C-D)) \times T_{sat} - D \times T)/C \tag{8}$$

$$C = \text{emissivity} \times \text{atmospheric transmittance} \tag{9}$$

$$D = (1 - \text{atmospheric transmittance})(1+(1-\text{emissivity}) \times \text{atmospheric transmittance} \tag{10}$$

where T_Q is the LST derived using the Qin, et. al. method, T_{sat} is the brightness temperature, and a, b are calibration constants, respectively.

Agro-meteorological data, whenever needed, were sourced from the Philippine weather bureau (PAGASA). Computation flowchart is shown below in Fig. 8. Table 1 gives the comparison matrix of these methods, summarizing the parameters and corrections used by each of the techniques.

Fig. 7, illustrates how LandSat 5 satellite readings are affected by environmental and system errors when observing LST. Sample environmental factors include cloud cover, haze due to cooling tower exhaust (from geothermal power plants) and burning of wood, water vapour in the atmosphere due to various evapo-transpiration processes, etc. Sample sources of system errors include satellite camera/sensor settings, satellite flight orientation, spatial resolution, and temporal resolution.

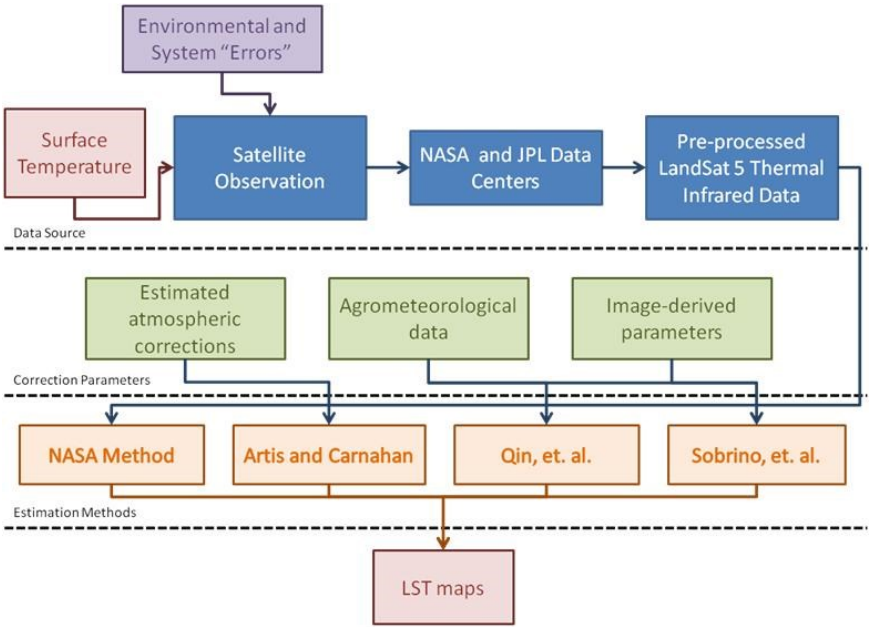

Fig. 8. Computation flowchart used in deriving the LST maps. Sobrino method (Jiménez-Muñoz, et al. 2009) will be implemented in future activities of this research.

Table 1. Comparison matrix of the methods used to derive the LST maps of LGBU. The importance of the input parameters, the corrections achieved in inputting the parameters, the limitations, and the advantages of the estimation methods are given in the columns.

Method	Input Parameters	Purpose	Limitations	Advantages
NASA	System constants found in the image metafile	Convert saved digital numbers (i.e. pixels values) back to spectral radiance estimates	1. More or less refers to blackbody reference only 2. If used on images that are not atmospherically corrected, method will not reflect ground conditions	1. Fast deployment 2. Easy to implement
Artis and Carnahan	Atmospheric correction from NASA's online facility	Provide additional corrections to account for atmospheric conditions at the time the image was observed	1. Empirical data used to estimate corrections are mostly from North America only 2. Over-estimates values over the study area	1. Uses atmospheric correction parameters that are commonly used in advanced computation software like MODTRAN
Qin, et. al.	Atmospheric transmittance and ground emissivity values from site-specific parameters	Correct for actual atmospheric and ground conditions at the time the image was observed	1. Needs local parameters from Philippine weather bureau which may not always be available 2. Different parameters are needed everytime there is a need to analyze a different location or site 3. Relatively difficult to implement	1. Takes into account local parameters in its computation 2. Gives the best estimate over LGBU 3. Parameters can be adjusted to account for the ground conditions at the site of interest

2.3 Verification of Results through Ground Observations

To complete the full Remote Sensing analysis and processing chain, and in order to verify the results of the image processing done on the two LandSat 5 images, in-situ observations were conducted at the study area. Twenty-five ground observations (Fig. 9) were done through thermocouple measurements. Despite constraints (i.e., safety, accessibility, etc.) sampling sites were tried to be as diverse and as well distributed as possible (i.e. grassy, barren, rice paddies, vegetated, etc.) (Fig. 10) to take into account different land cover and land use types inside the study area.

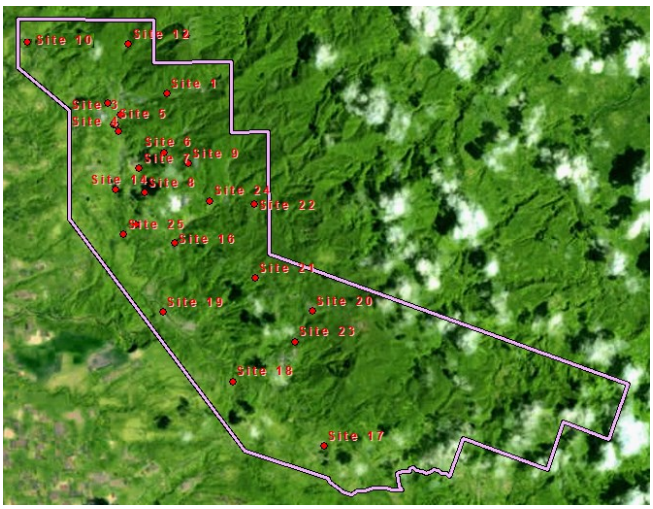

Fig. 9. Location of in-situ sampling sites at the study area. Observations were done by using a thermocouple.

Fig. 10. Sample observation sites. To take into account different land cover and land use types, observation sites included vegetated areas, rice paddies, and grassy areas nearby roads and pads.

Three temperature measurements were done at each sampling station, which include the air temperature, top soil temperature, and the ~1m deep bottom hole temperature. Fig. 11 shows the methodology used to get the measurements.

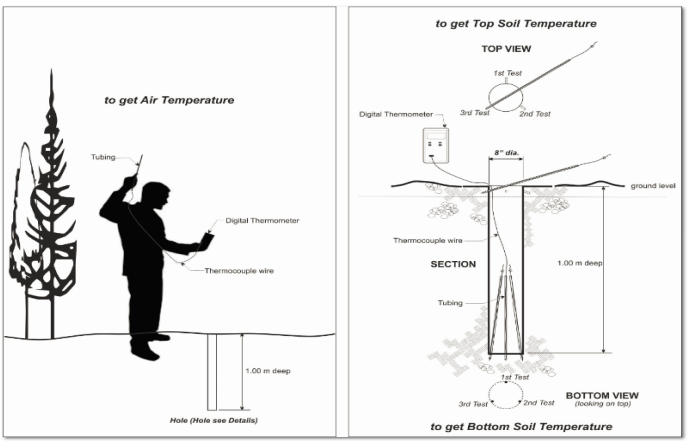

Fig. 11. Kinematic temperatures were observed by using a thermocouple. In-situ observations were then compared against those derived via thermal remote sensing.

3. COMPARISON OF LST MAPS DERIVED THROUGH REMOTE SENSING VERSUS IN-SITU TEMPERATURE OBSERVATIONS

To compare the differences between the satellite-derived values and in-situ measurements, statistical values were derived using each of the observations. These measures are shown in Table 2. A graph of the values was also plotted for visualization (Fig. 12).

From Table 2, and using the 2010 LandSat data as reference thermal image, the best methods to derive LST are those of NASA and Qin, et. al. with variances of just 1.49 and 1.52 deg °C respectively. The Artis and Carnahan method over estimated the LST (9.91 deg °C variance) for the study area because the upwelling and downwelling parameters used in Eq. 7 were from NASA. The modeling of the parameters might have not included in-situ/representative measurements from the Philippines and might not reflect the climate and weather at the study area.

Table 2. Averages, minimum, maximum, standard deviations, and variances of the differences of ground measurements versus satellite-derived values. Values in °C.

	1996_NASA_Diff	1996_Qin_Diff	2010_Artis_Diff	2010_NASA_Diff	2010_Qin_Diff
ave	3.90	4.45	10.26	1.28	1.74
min	0.15	0.70	1.36	0.01	0.15
max	7.96	8.59	15.66	6.19	6.00
std dev	1.65	1.73	3.15	1.23	1.22
var	2.73	3.00	9.91	1.52	1.49

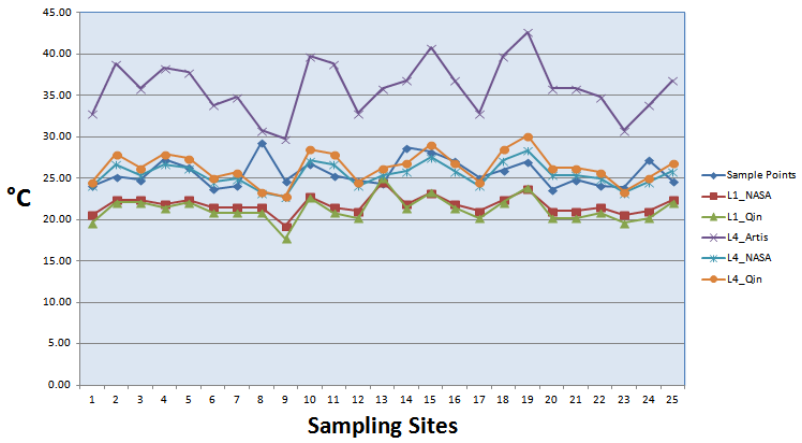

Fig. 12. Graph of differences in values between satellite-derived temperatures and in-situ thermocouple measurements. There is no Artis and Carnahan plot for the 1996 image because there are no available downwelling and upwelling radiance values (provided by NASA) for the 1996 image.

Fig. 12 also indicates that the 1996 LandSat image has an apparent systematic difference with in-situ measurements in terms of land surface temperature. This may reflect a manifestation of climate change at the study area, though this may need further analysis and is not the purpose of the paper. To avoid such cases, it may be worth considering to only use recent data (i.e. approx. 2009 above) when deriving LST maps.

Based on the statistical computations in Table 2, it can be deduced that Qin et. al.'s method, with its site specific parameters that deal with environmental factors like air temperature, humidity, moisture (i.e. climate and weather during the time of the observation of the satellite image), gives the best estimate of LST over the subject area.

4. CONCLUSIONS AND RECOMMENDATIONS

It was shown in this study that EDC can use thermal remote sensing in identifying areas where there is relatively high LST. The LST maps (Fig. 13) can be used in targeting areas for geothermal energy exploration where higher LST usually indicates locations of thermal anomalies, and possibly geothermal activity. This study also showed that LandSat datasets, despite its low spatial resolution (i.e. 30m – 60m), can be used for LST analyses since the satellite-derived temperature values are close to those measured on ground via thermocouple observations.

Using the most recent (i.e. 2010 image), almost cloud-free LandSat image over the study area, it was determined that the best methods to use when deriving LST maps are the Qin, et. al. mono-window algorithm and the NASA method. The variances are 1.49 deg C and 1.52 deg C and standard deviations are 1.22 deg C and 1.23 deg C, respectively.

However though the statistical values from the two methods appear almost equal, note that the temperature derived using the NASA method refers to a blackbody reference, hence it is theoretically incorrect. A blackbody is an idealized physical body that absorbs all incident electromagnetic radiation, regardless of frequency or angle of incidence; hence it does not represent actual ground conditions (i.e. leaves have different roughness and reflect sunlight differently compared to asphalt roads, etc.). Thus, whenever possible, the more appropriate method to use therefore is the Qin et. al. mono-window algorithm since the technique makes use of atmospheric corrections, agro-meteorological parameters, and takes into consideration ground surface emissivity.

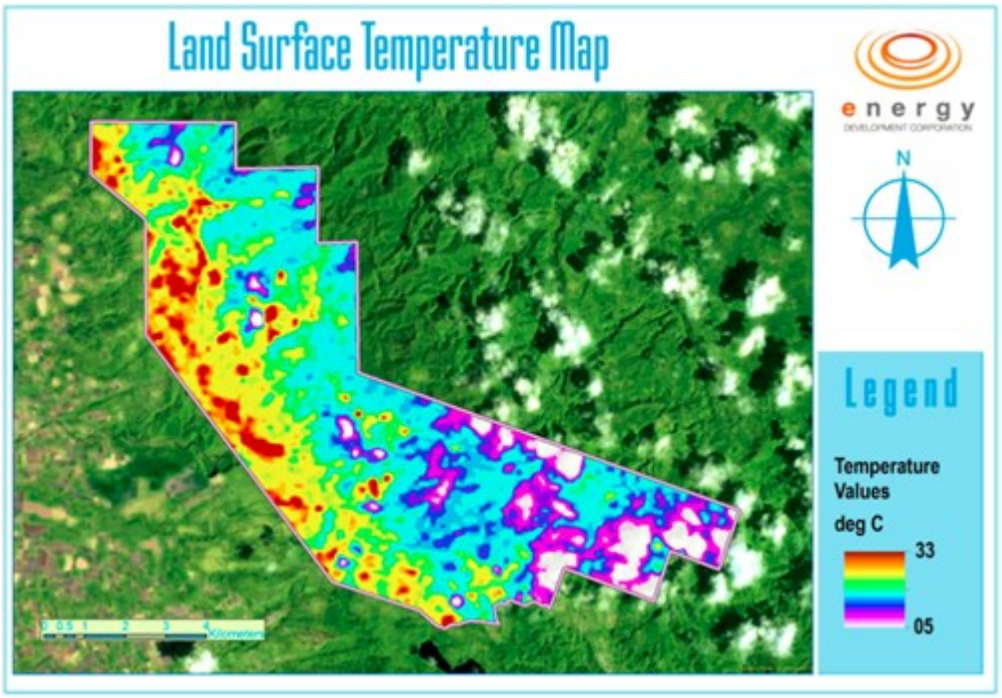

Fig. 13. Sample LST map derived for LGPF.

Incidentally, the study also revealed a considerable temperature difference (i.e. almost a systematic shift) between the 1996 image-derived LST values versus the ground measurements at the study area. Though a possible indicator of climate change, this still warrants further study and is beyond the scope of this paper.

The possibility of using higher resolution thermal images like the ASTER thermal imagery may be worth considering, owing to the promising results of the study. Higher resolution source data may provide correspondingly better quality, high-resolution LST maps compared to LandSat 5 thermal imageries that only provide temperature averaged over 30 to 60 sq. m. areas.

Future works include possible application of the Sobrino, et. al. single-channel algorithm (Jiménez-Muñoz, et al. 2009) for deriving LST (similar to Qin, et. al. algorithm), and geostatistical analysis of the LST maps vis-a-vis other geospatial information such as structural maps, geothermal anomaly maps, and digital elevation models to better identify geothermal prospect areas.

REFERENCES

Artis, D. A., and W. H. Carnahan. "Survey of emissivity variability in thermography of urban areas." *Remote Sensing of Environment* 12 (1982): 313-329.

Coolbaugh, M.F., C., A. Fallacaro, W.M. Calvin, and J.V. Taranik. "Detection of geothermal anomalies using Advanced Spaceborne Thermal Emission and Reflection Radiometer (ASTER) thermal infrared images at Bradys Hot Springs, Nevada, USA." *Remote Sensing of Environment*, 2007: 350-359.

Jiménez-Muñoz, Juan C., Jordi Cristóbal, José A. Sobrino, Guillem Sòria, Miquel Ninyerola, and Xavier Pons. "Revision of the Single-Channel Algorithm for Land Surface Temperature Retrieval From Landsat Thermal-Infrared Data." *IEEE Transactions on Geoscience and Remote Sensing* 47 (2009): 339-349.

NASA. "Landsat 7 Science Data Users Handbook." October 21, 2013. http://landsathandbook.gsfc.nasa.gov/ (accessed November 18, 2013).

Qin, Z., A. Karnieli, and P. Berliner. "A Mono-Window Algorithm for Retrieving Land Surface Temperature from Landsat TM Data and its applications to the Israel-Egypt Border." *Journal of Remote Sensing* 22 (2001): 3719-3746.

Shaply, Patricia. *Light and the Electromagnetic Spectrum.* 2012. http://butane.chem.uiuc.edu/pshapley/GenChem2/A3/3.html (accessed May 22, 2014).

Siahaan, Mona Natalia, Andri Soebandrio, and Ketut Wikantika. "Geothermal Potential Exploration Using Remote Sensing Technique Case Study: Patuha Area, West Java." *Asia Geospatial Forum.* Jakarta: Geospatial World, 2011.